Carboxylate Binding to Be^{2+} in Proteins and Influence of the Dielectric Environment

James A. Snyder*

Health Effects Laboratory Division, National Institute for Occupational Safety and Health, Centers for Disease Control and Prevention, Morgantown, West Virginia 26505-2888

Received: February 3, 2005; In Final Form: July 15, 2005

To gain insight into the interaction of Be^{2+} ions with negatively charged protein residues, the free energy changes associated with the replacement of water molecules in the first hydration shell of $Be(H_2O)_4^{2+}$ with one and two acetate anions were computed for the gas phase reactions using ab initio methods at the MP2 and DFT-B3LYP computational levels. Both unidentate and bidentate modes of coordination of the carboxylate group with the Be^{2+} ion are considered. Continuum dielectric calculations were then performed to estimate the corresponding free energy changes in several environments of varying dielectric strength. Environments with dielectric constants of 2 and 4, which represent a protein interior, and 78, which corresponds to water, were used. It is found that the free energy changes for the substitution reactions decrease in magnitude with increasing dielectric strength, in agreement with similar results reported for Mg^{2+}, Ca^{2+}, and Zn^{2+} (Dudev et al. *J. Phys. Chem. B* **2000**, *104*, 3692). However, unlike Mg^{2+}, Ca^{2+}, and Zn^{2+}, the free energy change for single-anion or *concerted* two-anion substitution reactions with $Be(H_2O)_4^{2+}$ remains negative and indicates the reactions are still favorable in the high dielectric aqueous environment. It is also found that the unidentate mode of binding is favored over the bidentate mode, and this is attributed, in part, to the introduction of hydrogen bonds between one carboxylate oxygen and a water molecule within the cluster when unidentate binding with Be^{2+} is involved.

Introduction

Among the group II metal ions, Mg^{2+} and Ca^{2+} are known to bind to many proteins with no measurable toxicological effect. However, the same is not true for Be^{2+}. An example might be found in chronic beryllium disease (CBD), which is a seriously debilitating, life threatening, occupational disease that occurs primarily among workers engaged in beryllium extraction and purification and the preparation of Be metal and its alloys. CBD is generally recognized to be preceded by immunologic sensitization involving histocompatibility complex (MHC) class II human leukocyte antigen (HLA) glycoprotein. Moreover, recent studies suggest that Be^{2+} may bind in the vicinity of Glu β69 of the protein coded by the HLA-DPB1 class of alleles, perhaps directly in the antigenic peptide binding groove.[1] Interaction of Be^{2+} with carboxylates of glutamate or aspartate residues in the protein requires transfer of the ion from aqueous solution to the low dielectric protein environment. The free energy change for this process can be examined by considering the substitution of a water ligand in the first solvation shell of the metal ion for a selectively chosen analogue of a carboxylate ligand.[2] In the present study, the acetate anion was used as the carboxylate analogue. Moreover, carboxylate ligands are observed to coordinate metal ions in either a *uni*dendate or *bi*dendate manner. Therefore, it is also of interest to compare energy differences between these two modes of coordination.

Methods

The reactions studied in this work are given in eqs 1−4:

$$Be(H_2O)_4^{2+} + nCH_3COO^- \rightarrow Be(CH_3COO)_{n,uni}(H_2O)_{4-n}^{(2-n)+} + nH_2O \qquad n = 1, 2 \quad (1)$$

$$Be(H_2O)_4^{2+} + nCH_3COO^- \rightarrow Be(CH_3COO)_{n,bi}(H_2O)_{4-2n}^{(2-n)+} + 2nH_2O \qquad n = 1, 2 \quad (2)$$

$$Be(CH_3COO)_{uni}(H_2O)_3^+ + CH_3COO^- \rightarrow Be(CH_3COO)_{2,uni}(H_2O)_2 + H_2O \quad (3)$$

$$Be(CH_3COO)_{bi}(H_2O)_2^+ + CH_3COO^- \rightarrow Be(CH_3COO)_{2,bi} + 2H_2O \quad (4)$$

For the case $n = 2$, reactions 1 and 2 infer a *concerted* replacement of two or four water molecules, respectively, with *two* acetate ions, whereas both reactions 3 and 4 depict the second replacement as a separate step. It should be noted that in each of these reactions the coordination number of Be^{2+} is always four. The coordination number for the Be^{2+} ion is most often observed to be four. A search using the Cambridge Structural Database found 144 beryllium structures, of which 98 had a beryllium coordination of four.[3] Be−O (N or S) bond distances were between 1.56 and 1.67 Å. Furthermore, molecular dynamics simulation predicts a coordination number of four in the first solvation shell of Be^{2+} ions positioned (as described below) around the HLA protein, near glutamate or aspartate residues, with Be−O distances in the aforementioned range. The coordination around the Be^{2+} ion in the complexes studied here mimics configurations found during molecular dynamics simulations of HLA proteins with Be^{2+} ions.

To contrast how free energy changes associated with the ligand substitution reactions given above are influenced by a

* Corresponding author. Phone: (304) 285-6364. Fax: (304) 285-6126. E-mail: zyu4@cdc.gov.

10.1021/jp050614w
Published on Web 08/27/2005

high dielectric medium such as water and a low dielectric environment simulating the interior of a protein, the procedure used by Dudev and Lim[2] was applied. Accordingly, free energy changes for reactions 1−4 in the gas phase at 298.15 K and 1 atm were computed on the basis of ab initio calculations at the MP2 and DFT-B3LYP levels using the 6-311G++(d,p) basis set. The Gaussian 98 program[4] was used for all ab initio calculations.

Starting geometries were derived from molecular dynamics snapshots of Be^{2+} coordinated with aspartate or glutamate side chains of an HLA protein solvated in a water box. There are no experimentally determined coordinates for HLA-DP in the Protein Data Bank (PDB; http://www.rcsb.org/pdb/). We modeled the extracellular part of HLA-DP by homology to a known HLA species.[5] All molecular dynamics (MD) simulations were performed using the CHARMM force field.[6] Each HLA-DP model contained 367 residues and was solvated using TIP3P water in an octahedral box. For the HLA-DPA1*01031 HLA-DPB1*1701 protein, 34 661 water molecules were added, and the box dimensions before truncation were 131.644 Å. The system was first subjected to 5000 steps of steepest descent minimization. The system was initially heated from 100 to 300 K for 15 ps in a CVT ensemble. Initial velocities were assigned on the basis of a Gaussian distribution of velocities at 100 K. This was followed by simulation in an NPT ensemble using the leapfrog integrator, and a langeven piston bath temperature of 298 K, using Hoover independent thermal piston coupling.[7] Long-range electrostatic interactions were treated using the particle-mesh Ewald (PME) summation method.[8,9] The nonbond cutoff was 10 Å. The SHAKE algorithm[10] was applied using a tolerance of 10^{-7} to fix bonds to hydrogen atoms. The C and C_α backbone atoms were restrained using a harmonic potential force constant of 500 kcal/mol. Each protein system was equilibrated for at least 1 ns.

Using the fully optimized geometries, molecular vibrational frequencies were computed at the MP2 and B3LYP levels and scaled by a factor of 0.9427 and 0.9613, respectively,[11] and these were used to estimate zero-point energies (ZPEs), thermal energies (E_T), and entropies (S). These values and the electronic energies (E_{elec}) were used to calculate Gibbs free energies for each complex and ligand in reactions 1−4, from which the free energy change for the *gas phase* ligand substitution reaction follows:

$$\Delta G_{sub}^{\epsilon=1} = \Delta E_{elec} + \Delta ZPE + \Delta E_T - T\Delta S \qquad (5)$$

Previous studies have suggested that the effect of basis set superposition error on the total energies of these complexes is insignificant.[2]

Using the ab initio optimized geometries, the free energy change for reactions 1−4 in an environment having a dielectric constant of x was computed by considering the following thermodynamic cycle:[2]

$$\begin{array}{ccc} \sum m_i A_i(\varepsilon=1) & \xrightarrow{\Delta G_{sub}^{\varepsilon=1}} & \sum m_j B_j(\varepsilon=1) \\ \sum m_i \Delta G_{solv}^{\varepsilon=x}(A_i) \downarrow & & \downarrow \sum m_j \Delta G_{solv}^{\varepsilon=x}(B_j) \\ \sum m_i A_i(\varepsilon=x) & \xrightarrow{\Delta G_{sub}^{\varepsilon=x}} & \sum m_j B_j(\varepsilon=x) \end{array} \qquad (6)$$

where $m_i\Delta G_{solv}^{\epsilon=x}(A_i)$ is the free energy change for the transfer of m_i molecules of reactant species A_i from the gas phase to an environment with a dielectric constant of x. The free energy change for the substitution reaction in an environment with a dielectric constant of x is then given by[2]

$$\Delta G_{sub}^{\epsilon=x} = \Delta G_{sub}^{\epsilon=1} + \sum m_j \Delta G_{solv}^{\epsilon=x}(B_j) - \sum m_i \Delta G_{solv}^{\epsilon=x}(A_i) \qquad (7)$$

$\Delta G_{solv}^{\epsilon=x}(A_i)$ was estimated using a continuum dielectric model. The electrostatic potential was calculated by numerically solving the linearized Poisson−Boltzmann equation using a finite difference method. The low dielectric solute ($\epsilon = 2$) was embedded in a dielectric continuum environment (exterior) with the dielectric constant set equal to 2, 4, or 78 in one calculation, and then, a second calculation was performed with the exterior dielectric constant equal to 1, to represent the gas phase. The difference in the electrostatic potentials provided the electrostatic free energy of solvation for the ligand or complex. The assigned temperature was 298 K. The solute boundary was defined by a solvent-accessible surface generated by a rolling probe sphere with a radius of 1.4 Å. The resulting system was discretized on a grid, and the potential at the grid points was solved iteratively starting from the Debye−Hückel boundary conditions. To improve the accuracy of calculated potentials, the method of grid focusing was used. This involved three additional calculations in which the molecule was allowed to occupy a successively larger fraction of the cubic grid volume so that values of the potential at the grid boundary could be calculated using the larger grid from each preceding calculation. The grid dimensions were selected to be 162 Å (spacing 2.70 Å/grid point), 92.4 Å (spacing 1.54 Å/grid point), 52.8 Å (spacing 0.88 Å/grid point), and 30.0 Å (spacing 0.50 Å/grid point). Natural bond orbitals (NBO) charges were used on the basis of the MP2 or B3LYP optimized geometries for each complex or ligand using the MP2 density. Initial values for radii were taken from Dudev and Lim[2] and adjusted to reproduce the free energy of solvation of acetate (−79.9 kcal/mol)[12] and Be^{2+} (−584 kcal/mol).[13] Be^{2+} was assigned a radius of 1.15 Å. The radii of carboxylate oxygen atoms were 1.50 Å, and the remaining radii were the same as that used in Dudev and Lim.[2] When the Lennard-Jones (LJ) parameters for the Be^{2+} cation were selected to be $\epsilon_{LJ} = 0.009$ kcal/mol and $\sigma_{LJ} = 0.9$ Å, respectively, the radial distribution function for the Be−O distance in the first hydration shell for a molecular dynamics simulation of Be^{2+} in water correctly reproduced the experimental value of 1.67 Å.[14] Because of the first hydration shell, the dielectric boundary for the metal complexes is sufficiently distant from the metal ion, such that the error in the solvation energy due to inaccuracies in the choice of a Born radius for the Be^{2+} ion becomes negligible.[2] In fact, the continuum dielectric calculations give identical results to two decimal places for the metal complexes for any choice of radius for Be^{2+} between 0.5 and 2.0 Å. The University of Houston Brownian Dynamics (UHBD) program[15,16] was used for the continuum dielectric calculations.

Results and Discussion

Table 1 gives the free energies calculated for reactions 1−4 for the various values of the dielectric constant (ϵ). Table 1 also lists the values of $T\Delta S_{sub}$ for $T = 298$ K for the gas phase, showing that the entropic term, although larger, as expected for reaction 2, comprises less than 4% of the free energy change. The MP2 free energy changes for reactions 1 and 2 are plotted as a function of ϵ in Figure 1. Overall, the results of the MP2 and B3LYP calculations appear quite similar. A discussion on sources of error can be found elsewhere.[2]

As Table 1 and Figure 1 show, the magnitude of the free energy changes decreases with increasing dielectric strength. Similar results were found for the substitution reactions with the hydrated complexes of Mg^{2+}, Ca^{2+}, and Zn^{2+}.[2] The similarity of the trend in the free energy changes can be seen

TABLE 1: Free Energy and Entropy Changes (kcal/mol) for the Substitution of *n* or 2*n* Water Molecules for *n* Acetate Anions (Reactions 1−4 in Text) in the First Hydration Shell of $Be(H_2O)_4^{2+}$

	$T\Delta S_{sub}^{\epsilon=1}$		$\Delta G_{sub}^{\epsilon=1}$		$\Delta G_{sub}^{\epsilon=2}$		$\Delta G_{sub}^{\epsilon=4}$		$\Delta G_{sub}^{\epsilon=78}$	
reaction	MP2	B3LYP	MP2	B3LYP	MP2	B3LYP	MP2	B3LYP	MP2	B3LYP
1, $n=1$	−2.6	−2.7	−242.0	−240.7	−131.1	−130.0	−77.9	−77.0	−31.3	−30.5
2, $n=1$	9.1	6.1	−227.6	−223.2	−120.9	−117.0	−70.2	−66.5	−25.8	−22.1
1, $n=2$	−5.2	−6.8	−378.1	−371.9	−201.9	−195.8	−113.7	−107.6	−30.3	−24.4
2, $n=2$	13.9	12.4	−358.8	−353.2	−186.6	−180.6	−101.3	−95.0	−21.8	−15.1
3	−2.6	−3.4	−136.1	−131.9	−70.9	−66.5	−35.8	−31.3	1.0	5.5
4	4.8	6.9	−131.2	−130.6	−65.7	−64.4	−31.1	−29.2	4.0	6.4

in Figure 1 which shows that the decrease in magnitude is faster at low dielectric strengths, and the values approach zero with increasing ϵ. However, in the case of $Be(H_2O)_4^{2+}$, the free energy changes predicted in this study for the reaction of one acetate anion or the *concerted* reaction of *two* acetate anions are found to be negative for all values of ϵ. This implies that the substitution reactions are favorable, even in the high dielectric ($\epsilon = 78$) medium. This can be compared with results found for Mg^{2+}, Ca^{2+}, and Zn^{2+}, by Dudev and Lim,[2] for which the substitution of one water molecule for a formate anion is

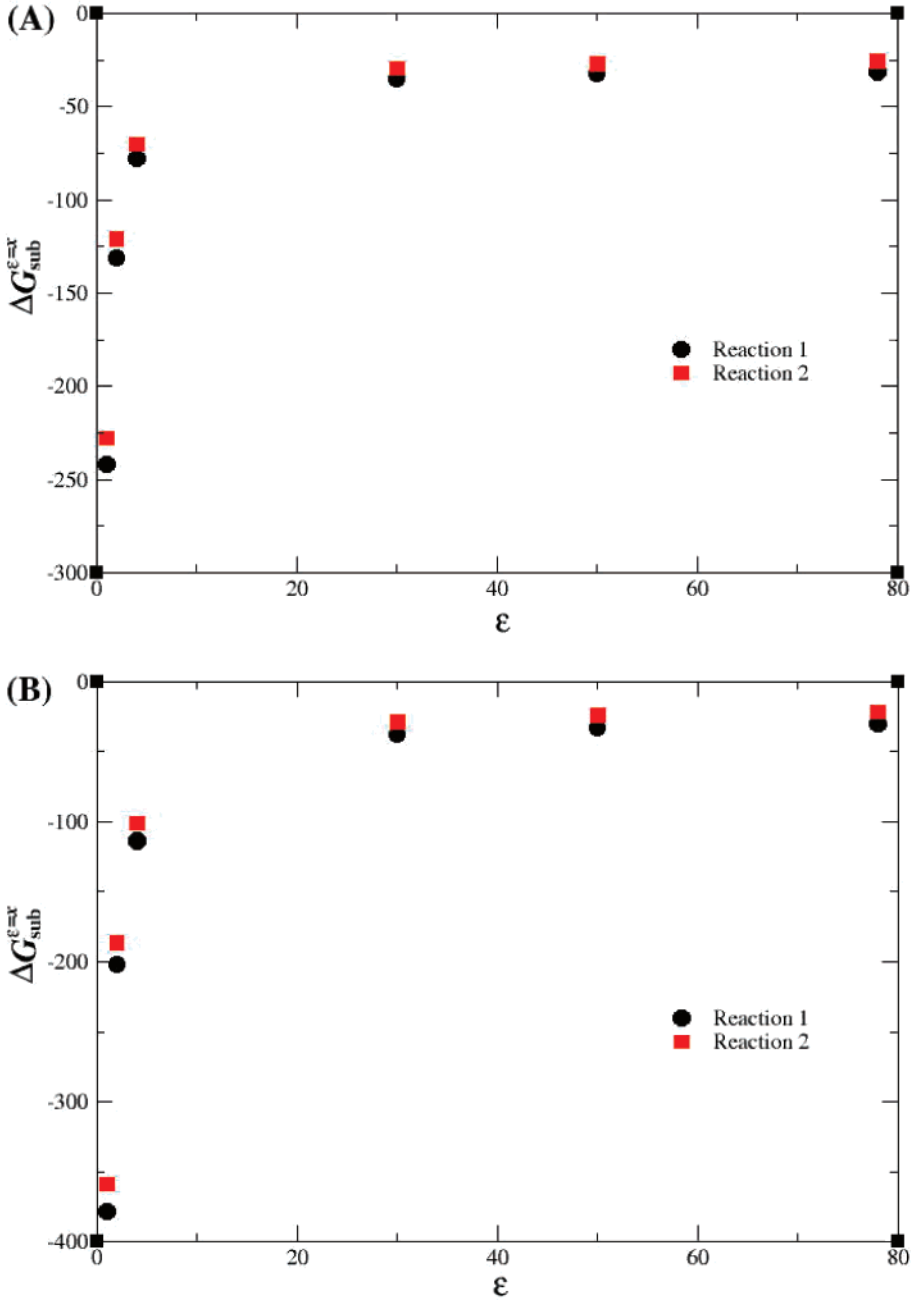

Figure 1. Plot of the MP2 free energy of substitution ($\Delta G_{sub}^{\epsilon=x}$, kcal/mol) versus dielectric strength (ϵ) for reactions 1 and 2 for the substitution of (A) $n = 1$ and (B) $n = 2$ acetate anions.

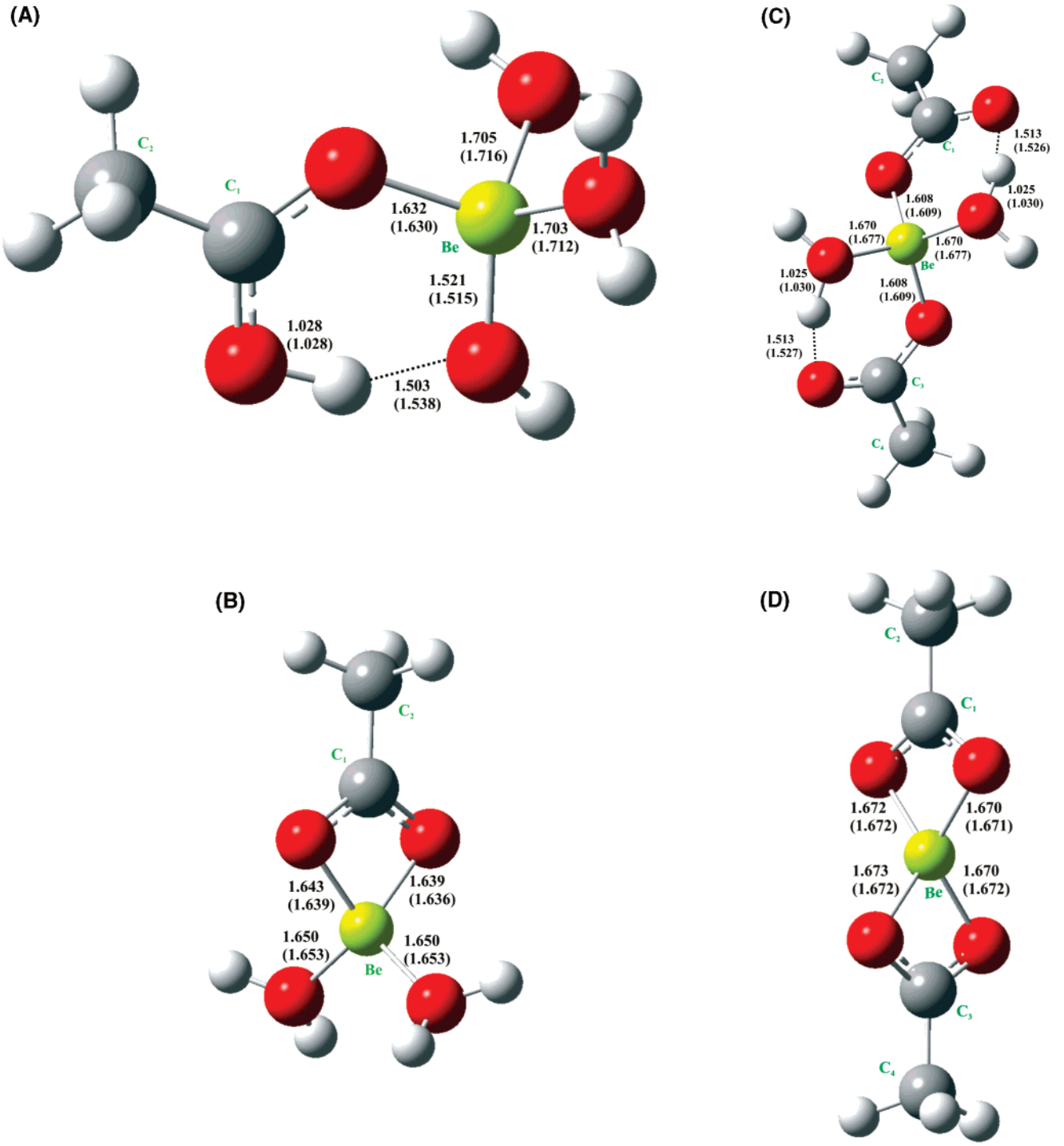

Figure 2. Geometries of Be^{2+} water/acetate clusters optimized at the MP2 level of computational theory: (A) $Be(H_2O)_3(CH_3COO)^+$; (B) $Be(H_2O)_2(CH_3COO)^+$; (C) $Be(H_2O)_2(CH_3COO)_2$; (D) $Be(CH_3COO)_2$. The values in parentheses are bond distances from DFT-B3LYP optimization.

predicted to be unfavorable in high dielectric environments, which was interpreted to mean that ligand substitution was restricted to solvent excluded cavities within the protein interior.

Table 1 indicates that the free energy changes for reactions 3 and 4 are positive in the $\epsilon = 78$ environment. Hence, although a *concerted* substitution of water for *two* acetate anions is favorable, the *stepwise* substitution is not. In aqueous solution, the concerted replacement reaction would require the simultaneous interaction of two acetate ligands with $Be(H_2O)_4^{2+}$ and each in the correct orientation for exchange. Although the probability of this event may be small in the aqueous solution, it is conceivable that a protein may present an environment in which two carboxylate groups are geometrically poised for such a *concerted* replacement and may even, to some extent, catalytically promote the substitution reaction.

The data in Table 1 and Figure 1 also indicate that the unidentate mode of binding (reaction 1) is favored compared to bidentate binding (reaction 2) by as much as −14 and −19 kcal/mol (MP2 values) for the reaction of one and two acetate anions ($n = 1$ and 2), respectively, in the gas phase ($\epsilon = 1$). However, the differences become smaller as the dielectric strength of the environment increases, becoming approximately −6 and −9 kcal/mol, respectively, at $\epsilon = 78$. This suggests that preferential binding in the unidentate mode for Be^{2+} is

perhaps more important in low dielectric solvent excluded cavities. Evidently, the entropy changes for reaction 1 involving the unidendate binding of an acetate anion are negative in the gas phase, probably due to the introduction of hydrogen bond(s) (Figure 2) which may off-set the positive entropy effect associated with the loss of a water molecule(s) from the first shell. Hence, although the free energy change for reaction 1 is more favorable compared to reaction 2 by −14 ($n = 1$) and −19 ($n = 2$) kcal/mol, the differences between the entropy changes for reactions 1 and 2 are, according to Table 1, −12 ($n = 1$) and −19 ($n = 2$) kcal/mol (MP2) and are unfavorable. By comparison, the entropy change for the replacement of a water molecule with a unidendate bound formate ligand was reported to be positive for Mg^{2+},[2] which may be due to a weaker hydrogen bond in the hydrated complexes of the larger ions.

Figure 2 shows the optimized geometries for the complexes with the acetate anion(s) bound in a unidentate mode (Figure 2A and C) and in a bidentate mode (Figure 2B and D). The Be−O distances are also presented for both the MP2 and B3LYP results. Also shown are H−A distances of hydrogen bonds between the H atom of water and the acceptor oxygen atom of acetate. As Figure 2A shows, the binding of the acetate anion in a unidentate mode allows one oxygen atom of the anion to act as a proton acceptor for a hydrogen bond with a nearby water molecule within the complex. For the hydrogen bond in the monoanion complex in Figure 2A, the B3LYP values for the H−A distance and the donor (water) oxygen−acceptor oxygen distance are 1.538 and 2.506 Å, respectively. In a DFT calculation on the $Be(H_2O)_3(acetate)^+$ complex using the 6-31+G* basis set and the B3LYP functional, the corresponding values were found to be 1.440 and 2.454 Å, respectively.[3] Comparison of part A with part B and part C with part D of Figure 2 shows that the Be−O distances for the ligated oxygens of the acetate anion are shorter in the unidentate complex compared with those of the bidentate complexes. However, the Be−O distances for the two remaining water molecules are slightly longer in Figure 2A (e.g., 1.703 and 1.705 Å, MP2) compared to Figure 2B (1.650 Å). The hydrogen bond donor and acceptor atoms and distances are reversed in the dianion complex in Figure 2C (the H atom is closer to the water) when compared with the monoanion complex in Figure 2A. However, according to Table 1, the differences between the free energy changes for reaction 2 compared to 1 for $n = 2$, which involves the disruption of two hydrogen bonds, are greater compared with the disruption of only one hydrogen bond ($n = 1$).

Conclusion

Comparison of the calculated free energy changes for the substitution of one and two acetate anions for water molecules in the first hydration shell of Be^{2+} indicates that the monodendate mode of ligand binding is favored by the acetate anion. The free energy changes become smaller in magnitude as the dielectric constant of the environment increases. However, for substitution involving one acetate ion, unlike the case for Mg^{2+}, Ca^{2+}, and Zn^{2+}, the free energy changes do not become positive in a high dielectric environment ($\epsilon = 78$). Free energy changes for *concerted* substitutions of *two* acetate ions are also negative in the high dielectric environment but become positive for the second replacement when the substitutions are considered as *stepwise* reactions. These findings may be useful for interpretation of molecular modeling results of the interaction of Be^{2+} ions with proteins such as HLA. The region of the protein where the metal ion may bind may provide a unique environment. If, for example, a comparison is made of binding energies for the metal ion at different sites on the protein, it may prove insightful to compare the results with the energies reported here to predict the extent to which the protein uniquely effects the substitution reaction.

Acknowledgment. The author wishes to thank the National Cancer Institute's Advanced Biomedical Computing Center (NCI-ABCC) for the use of their computational facilities. The findings and conclusions in this report are those of the author and do not necessarily represent the views of the National Institute for Occupational Safety and Health.

References and Notes

(1) Amicosante, M.; Sanarico, N,; Berretta, F.; Arroyo, J.; Lombardi, G.; Lechler, R.; Colizzi, V.; Saltini, C. 2001. *Hum. Immunol.* **2001**, *43*, 686.

(2) Dudev, T.; Lim C. *J. Phys. Chem. B* **2000**, *104*, 3692.

(3) Scott, B. L.; Wang, Z.; Marrone, B. L.; Sauer, N. N. *J. Inorg. Chem.* **2003**, *94*, 5.

(4) Frisch, M. J.; Trucks, G. W.; Schlegel, H. B.; Scuseria, G. E.; Robb, M. A.; Cheeseman, J. R.; Zakrzewski, V. G.; Montgomery, J. A.; Stratmann, R. E., Jr.; Burant, J. C.; Dapprich, S.; Millam, J. M.; Daniels, A. D.; Kudin, K. N.; Strain, M. C.; Farkas, O.; Tomasi, J.; Barone, V.; Cossi, M.; Cammi, R.; Mennucci, B.; Pomelli, C.; Adamo, C.; Clifford, S.; Ochterski, J.; Petersson, G. A.; Ayala, P. Y.; Cui, Q.; Morokuma, K.; Malick, D. K.; Rabuck, A. D.; Raghavachari, K.; Foresman, J. B.; Cioslowski, J.; Ortiz, J. V.; Baboul, A. G.; Stefanov, B. B.; Liu, G.; Liashenko, A.; Piskorz, P.; Komaromi, I.; Gomperts, R.; Martin, R. L.; Fox, D. J.; Keith, T.; Al-Laham, M. A.; Peng, C. Y.; Nanayakkara, A.; Gonzalez, C.; Challacombe, M.; Gill, P. M. W.; Johnson, B.; Chen, W.; Wong, M. W.; Andres, J. L.; Gonzalez, C.; Head-Gordon, M.; Replogle, E. S.; Pople, J. A. *Gaussian 98*, revision A.7; Gaussian, Inc.: Pittsburgh, PA, 1998.

(5) Snyder, J. A.; Weston, W.; Tinkle, S.; Demchuk, E. *Environ. Health Perspect.* **2003**, *111* (15), 1827−1834.

(6) Brooks, B. B.; Broccoleri, R. E.; Olafson, B. D.; States, D. J.; Swaminathan, S.; Karplus, M. CHARMM: a program for macromolecular energy, minimization and dynamics calculations. *J. Comput. Chem*. **1983**, *4*, 187−217.

(7) Hoover, W. G. *Phys. Rev. A* **1985**, *31* (3), 1695.

(8) Darden, T.; York, D.; Pedersen, L. Particle mesh Ewald−an Nlog(N) method for Ewald sums in large systems. *J. Chem. Phys.* **1993**, *98*, 10089−10092.

(9) Essmann, U.; Perera, L.; Berkowitz, M. L.; Darden, T.; Lee, H.; Pedersen, L. G. A smooth particle mesh Ewald method. *J. Chem. Phys.* **1995**, *103*, 8577−8593.

(10) Ryckaert, J.-P.; Ciccotti, G.; Berendsen, H. J. C. Numerical integration of the Cartesian equations of motion of a system with constraints: Molecular dynamics of *n*-alkanes. *J. Comput. Phys.* **1977**, *23*, 327−341.

(11) Wong, M. W.; Wiberg, K. B.; Frisch, M. J. *J. Chem. Phys.* **1991**, *95*, 8991.

(12) Kang, K. K.; Némethy, G.; Scheraga, H. A. *J. Chem. Phys.* **1987**, *91*, 4118.

(13) Burgess, J. *Metal Ions in Solution*; Ellis Horwood: Chichester, England, 1978.

(14) Yamaguchi, T.; Ohtaki, H.; Spohr, G.; Pálinkás, K.; Heizinger, M. M. *Z. Naturforsch.* **1986**, *41a*, 1175.

(15) Davis, M. E.; Madura, J. D.; Luty, B. A.; McCammon, J. A. *Comput. Phys. Commun.* **1991**, *62*, 187.

(16) Madura, J. D.; Briggs, J. M.; Wade, R. C.; Davis, M. E.; Luty, B. A.; Ilin, A.; Antosiewicz, J.; Gilson, M. K.; Bagheri, B.; Scott, L. R.; McCammon, J. A. *Comput. Phys. Commun.* **1995**, *91*, 57.